Outer Membrane Vesicles Secreted by *Bacteroides fragilis* Inhibit CFTR Chloride Secretion by Human Colon Organoids

Roxanna Barnaby[1]*, Amanda Nymon[1]*, Paige Salerno[1]*, Carolyn Roche[1], Young Ah Goo[3], Byoung-Kyu Cho[3], Timothy B. Gardner[2], Zdenek Svindrych[4], Douglas J. Taatjes[5], Thomas H. Hampton[1], Benjamin Ross[1] and Bruce A. Stanton[1**]

[1]Department of Microbiology and Immunology, Geisel School of Medicine at Dartmouth, Hanover, NH, USA, [2]Center for Digestive Health, Dartmouth Hitchcock Medical Center, Lebanon, NH USA, [3]Mass Spectrometry Technology Access Center, McDonnell Genome Institute, Washington University School of Medicine, St. Louis, Missouri, USA, [4]Department of Biochemistry and Cell Biology, Geisel School of Medicine at Dartmouth, Hanover, NH, USA, and [5]Department of Pathology and Laboratory Medicine, University of Vermont, Burlington, VT USA

***Co-first authors.**

****Corresponding author:**

Bruce A. Stanton, Ph.D.
Department of Microbiology and Immunology
Geisel School of Medicine at Dartmouth
520 Remsen Building
Hanover NH 03755
Phone: 603-229-2803
Email: bas@dartmouth.edu

Running title: *Bacteroides Fragilis* toxin

Competing interests. The author(s) declare no competing interests.

Abstract. The goals of this study were to develop a model to study host pathogen interactions in primary human colon cells and to test the hypothesis that *Bacteroides fragilis* toxin (BFT) secreted in outer membrane vesicles (OMVs) modulates mucosal immunity and CFTR Cl^- secretion. Since Bacteroides species often resides in mucus, OMVs are likely to represent a mechanism of communication between Bacteroides and the host. Two strains of Bacteroides were studied, Enterotoxigenic *Bacteroides fragilis* (ETBF), which produces BFT, and the non-toxigenic *Bacteroides fragilis* strain NCTC 9343 (NTBF) that does not express *bft*. We also utilized two additional strains of *Bacteroides fragilis:* one in which *bft* was knocked out (ETBF Δ*bft*), and one that was engineered to contain *bft* (NTBF+*bft)*. We report that most *Bacteroides fragilis* OMVs reduced forskolin-stimulated CFTR Cl^- secretion, but had no effect on tight junction or cell adhesion structure, transepithelial resistance or the innate immune response of primary human colon monolayers. BFT did have an adverse effect on CFTR Cl^- secretion, but other factors in OMVs also inhibited CFTR Cl^- secretion. We conclude that OMVs secreted by Bacteroides can be an important mechanism of host pathogen interactions in the colon by reducing CFTR Cl^- secretion.

Keywords: *Bacteroides fragilis*, outer membrane vesicles, OMV, CFTR, colonoids

Introduction. The human gastrointestinal tract is colonized by ~100 trillion bacteria, including several members of the genus Bacteroides which comprise approximately thirty percent of the microbiota [1-5]. Although *Bacteroides fragilis* (*B. fragilis*) is one of the least abundant species,

48 Enterotoxigenic *B. fragilis* (ETBF) is a commensal bacterium that induces diarrhea, colitis and
49 causes tumor formation through the secretion of Bacteroides fragilis toxin (BFT), a
50 metalloprotease [3,6-8]. Many studies on colon cell lines have shown that recombinant BFT rapidly
51 (~1 hour) causes cell damage and disrupts cell adhesion structure by cleaving E-cadherin
52 leading to an increase in epithelial paracellular permeability, IL-8 secretion [3,9,10], fluid secretion
53 driven by CFTR Cl^- channels [11,12] and diarrhea [13-15]. Moreover, it has been suggested that the
54 BFT-induced increase in permeability leads to paracellular movement of bacteria and bacterial
55 products from the lumen of the colon to the submucosal layer and blood, an effect that can train
56 the immune system [2]. Recombinant BFT applied to the apical side of HT 29/C1, HT-29, T84,
57 the mouse colon epithelial cell line CMT93 or MDCK cell lines decreases transepithelial
58 resistance (TER) and cleaves the cell adhesion protein E-cadherin [9,13,15-17]. One study on a
59 colon cell line reported no effect of BFT on short circuit current but did report that BFT reduced
60 TER [17]. Since many Gram negative bacteria, including *B. fragilis,* secrete outer membrane
61 vesicles (OMVs) [18-24] that stimulate inflammation and decrease ion transport, including CFTR Cl^-
62 secretion by epithelial cells [18-20,25] communication between *B. fragilis*, which resides in mucus,
63 and the colon is likely, at least in part, to be mediated by the secretion of OMVs and other
64 soluble factors [7,26,27]. *B. fragilis* secretes OMVs containing BFT that cause epithelial cell
65 disruption and a time-dependent degradation of E-cadherin in the HT-29 cell line [24]. Notably,
66 BFT has been shown to reside on the surface of OMVs [24]. However, nothing is known about the
67 effects of BFT-containing OMVs secreted by *Bacteroides* on the biology of monolayers of
68 primary human colon organoids.

69 In contrast to ETBF, the Nontoxigenic *B. fragilis* (NTBF) strain does not express *bft* and it
70 promotes gut homeostasis through the production of short-chain fatty acids and
71 polysaccharide A, stimulates barrier-protective molecules including ZO-1 and MUC-2,
72 as well as the secretion of antimicrobial peptides, and anti-inflammatory cytokines [1,7,28].

73 A recent review suggested that cell lines are poor models to elucidate the physiology and
74 pathophysiology of the colon since cell lines are rarely normal, and contain several mutations
75 and chromosomal defects that enable their persistence [29]. In particular it has been reported that
76 the gene expression pattern of the Caco-2 cell line, which is studied as a surrogate of the colon,
77 was similar to that of epithelial cells of the small intestine [30]. Thus, one of the most important
78 challenges involve the accurate assessment of BFT's biological activity on relevant cells types [1].
79 To elucidate the biological activity of BFT secreted in OMVs, our studies obtained colon
80 biopsies from multiple healthy human donors to develop differentiated two-dimensional
81 monolayers of primary colon organoids. Colon organoids better mimic the natural tissue
82 environment, preserving the different cell populations and differentiation stages found in native
83 tissue, compared to cell lines which do not fully differentiate [29]. To the best of our knowledge no
84 studies have examined the biological effect of OMVs containing BFT secreted by *B. fragilis* on
85 primary human colon cells. Therefore, the goals of this study were to develop a model to study
86 host pathogen interactions in primary human colon cells and to test the hypothesis that BFT
87 secreted in OMVs modulates mucosal immunity and CFTR Cl^- secretion, a major driver of fluid
88 secretion in the colon [12]. We report that OMVs had no effect on cell adhesion or tight junction
89 proteins, notably E-cadherin and claudin-2, respectively or on TER, but did inhibit forskolin-
90 stimulated CFTR Cl^- secretion, an effect predicted to decrease fluid secretion by the colon. In
91 addition, OMVs were not pro-inflammatory as determined by measuring the secretion of 48
92 cytokines. OMVs also reduced CFTR Cl^- secretion by T84 cells, a colon cell line but did not alter
93 TER. These results demonstrate that OMVs secreted by *B. fragilis* have very different biological
94 effects on primary human colon organoids and T84 cells compared to the response of cell lines
95 to recombinant BFT.

96 **Results**

97 **Isolation and characterization of OMVs secreted by Bacteroides.** To test the hypothesis
98 that BFT in OMVs leads to a disruption in the integrity of epithelial barriers and modulates CFTR
99 Cl^- secretion, we utilized four strains of *B. fragilis*, including ETBF and ETBF in which the *bft*
100 gene was deleted (ETBF Δ*bft*), NTBF, a strain that does not express *bft,* and NTBF in which the
101 *bft* gene was expressed (NTBF+*bft*). Nanoparticle tracking analysis (NTA) revealed that the size
102 (130 nm) and concentration of OMVs isolated from cell culture media ($1.4x10^{11}$ for ETBF,
103 $2.8x10^{11}$ for ETBF Δ*bft,* $2.0x10^{11}$ for NTBF and $2.2x10^{11}$ for NTBF+*bft*) were similar across all
104 strains. To confirm that we isolated OMVs, transmission electron microscopy was utilized
105 (**Figure 1**). OMVs were not observed in process control (PC, cell culture media not exposed to
106 cells and run through the OMV isolation process); however, OMVs with typical morphology were
107 observed in media isolated from ETBF (**Figure 1**).

108 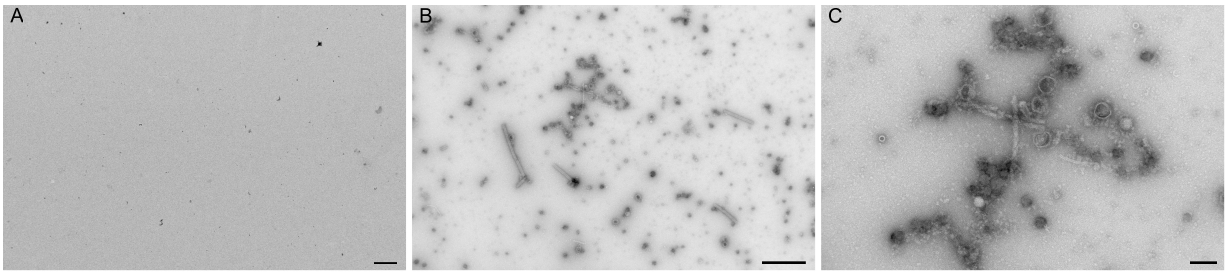

109 **Figure 1. Representative transmission electron microscopy images of negatively stained**
110 **OMVs.** (A) Process control. Scale bar 500 nm. (B) ETBF, Scale bar 500 nm. (C) The same
111 image as B, but at a higher magnification to visualize OMVs. Scale bar 100 nm.

112

113 Analysis of the proteome of OMVs was conducted to confirm that BFT was present in ETBF and
114 absent in NTBF. Detailed results of the proteomics analysis of OMVs are presented in
115 Supplemental Tables 1-4 and **Figure 2**. We detected 568 proteins in NTBF OMVs and 437
116 proteins in ETBF OMVs, with 247 proteins being found in both strains. BFT was detected in
117 ETBF OMVs and was absent in NTBF OMVs, as expected. qPCR confirmed the presence of *bft*

118 in NTBF+*bft*; however, *bft* could not be detected in NTBF and ETBF Δ*bft* (data not shown).
119 Fragipain was not detected in any of the samples (Supplemental Table 4.2). Fragipain is known
120 to cleave BFT into its active form [31], however, studies suggest that this protein is not required to
121 cleave BFT in antibiotic treated mice [32]. More specifically, fragipain is unnecessary when
122 purified BFT is mixed with the colon mucus of pathogen free or germ-free mice, suggesting the
123 mucosal activation process may be more prevalent in gastrointestinal conditions containing
124 increased mucus, such as CF [32]. The same study showed evidence that implies BFT mixed with
125 PBS is also capable of being cleaved into its active form, which raises the question of auto-
126 cleavage and further suggesting fragipain is not required for BFT activation [32]. Importantly, as
127 demonstrated below, *B. fragilis* colonoids secrete mucus. Taken together, the presence of BFT
128 but absence of fragipain in our proteomics did not deter us from further investigation of the
129 effects of BFT in this study.

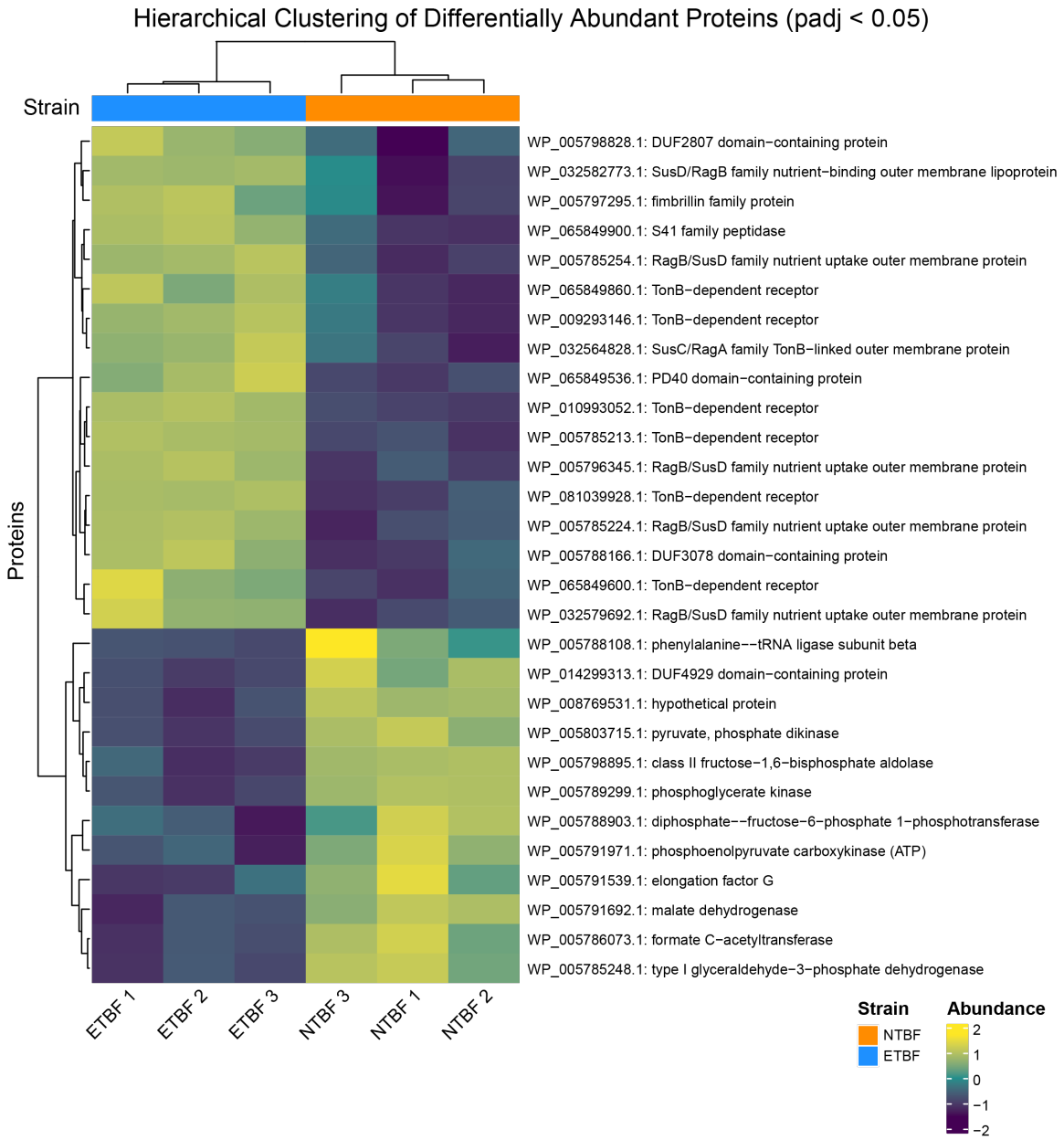

Figure 2. ETBF and NTBF OMV proteomes. Differential abundance analysis reveals significant differences between the shared proteome of ETBF and NTBF OMVs. The list of identified proteins by proteomics analysis are presented in Supplemental Tables 1-4. Supplemental Table 1 includes proteins detected exclusively in NTBF OMVs. Supplemental Table 2, includes proteins detected exclusively in ETBF OMVs. Supplemental Table 3, includes proteins detected in both ETBF and NTBF OMVs. Finally, Supplemental Table 4, includes

137 differential expression of proteins in ETBF and NTBF OMVs, the results of which are depicted in
138 this Figure.

139

140 In accordance with previous research, our results show several TonB dependent receptors are
141 more abundant in OMVs secreted by ETBF compared to NTBF strains (Supplemental Table 4)
142 [33]. TonB dependent receptors are one part of outer membrane structures that are critical for the
143 influx of nutrients via SusC and SusD outer membrane proteins, which were also shown to be
144 increased in ETBF OMVs [34]. An increase in abundance of these proteins suggests an increased
145 need for ETBF to enhance nutrient acquisition, thereby improving its ability to compete for
146 similar niches that NTBF does not struggle to fill. Regardless, these results pose interesting
147 questions for mechanistic follow up experiments in the future.

148 **Characterization of human colon organoids: Development of a model to study host**
149 **pathogen interactions in the colon.** Biopsies of proximal colon were obtained during
150 colonoscopy after obtaining informed consent from healthy volunteers. As described in methods
151 crypt cells were dispersed and grown in Matrigel until 3D organoids were formed. 3D organoids
152 were then seeded on Transwell filters and grown for one week to develop polarized, and
153 differentiated two dimensional (2D) monolayers. We used an imaging approach to characterize
154 the cellular composition of colon cells *in vitro* as 2D monolayers. **Figures 3-4** reveal that the
155 colon organoids contain cell types found in the proximal colon including mucin (MUC2)
156 producing cells, CFTR expressing cells, SLC26A3 (DRA, a Cl^-/HCO^-_3 exchanger that plays a
157 key role in fluid absorption and enterocyte acid/base balance) expressing cells and
158 enterochromaffin cells that underlie epithelial cells and secrete serotonin which stimulates GI
159 motility and fluid and electrolyte secretion [12,35]. These observations indicate that the human
160 primary 2D colon organoids are a well differentiated epithelium, have similar cell types to colon
161 *in vivo* and thus are a good model to study host pathogen interactions [12,35].

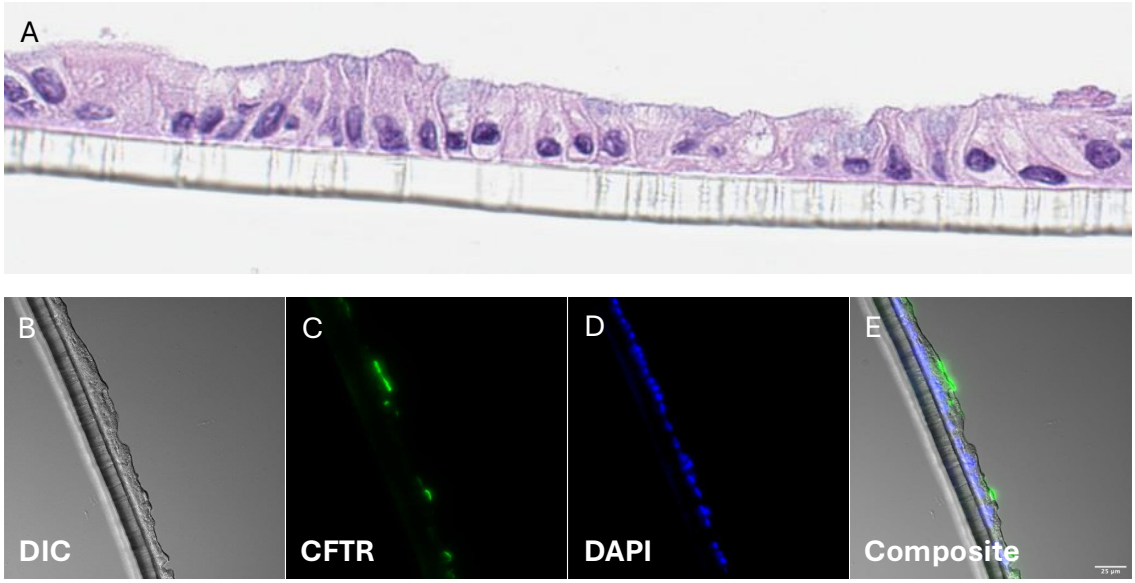

Figure 3. Representative images of human colon organoids. (A) Cross section of a confluent monolayer of colon organoids grown on Transwell filters (10 μm thick: H&E-stained cells). (B) differential contrast (DIC) image of a 6 μm thick frozen cross-section of differentiated colon organoids on Transwell filters. (C) Image of same organoid as in B but immunofluorescent image of CFTR. (D) DAPI nuclear labeling of the same organoid monolayer as in B and C. (E) Composite of B-D showing apical membrane labeling of CFTR. Scale bar 50 μm.

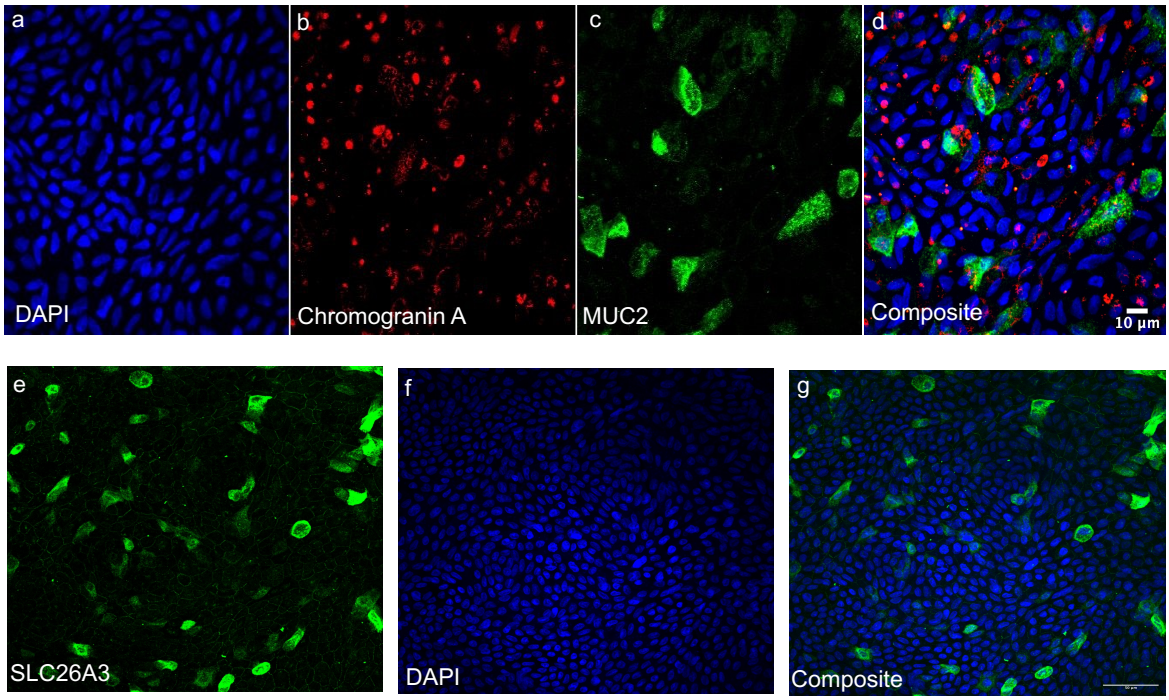

Figure 4. Representative *en face* images of 2D human colon organoids on Transwell filters. (a) DAPI labeling of nuclei. (b) Chromogranin A immunofluorescence of enterochromaffin cells. (c) Immunofluorescence of MUC2. (d) Composite of A-C revealing that MUC2 and Chromogranin A are expressed in different cell types. (e) Immunofluorescence of SLC26A3 (DRA, a Cl^-/HCO^-_3 exchanger). (f) DAPI labeling of nuclei. (g) Composite of e and f. Scale bar in g is 50 μm.

OMVs inhibit CFTR Cl^- secretion by primary human colon organoids. Previous studies have shown that recombinant BFT purified by chromatography stimulates short circuit current, which is indicative of Cl^- secretion, when added to the basolateral side of T84 cells [17]. To examine the effect of OMVs secreted by *B. fragilis* on CFTR Cl^- secretion by primary human colonoids, OMVs were isolated and applied to the apical side (the side of the colon exposed to Bacteroides in vivo) of colon organoids for 1 hour and then forskolin-stimulated CFTR Cl^- secretion was measured in Ussing chambers immediately after the 1 hour exposure, or 24

185 hours after washing the OMVs from the organoids. **Figure 5** demonstrates that OMVs secreted
186 by ETBF, ΔETBF and NTBF+*bft* reduced forskolin stimulated CFTR Cl^- secretion after 1 hour of
187 exposure (statistical significance in figure legend) compared to PC. Notably, OMVs secreted by
188 ETBF reduced Cl^- secretion significantly more than OMVs secreted by NTBF that does not
189 express BFT. Deletion of endogenous *bft* from ETBF reduced the inhibitory effect of ETBF
190 OMVs on CFTR Cl^- secretion. OMVs secreted by NTBF+*bft* inhibited CFTR Cl^- secretion more
191 that NTBF OMVs, which do not express BFT. Taken together, these data show that 1 hour
192 exposure to OMVs secreted by *B. fragilis* reduces CFTR Cl^- secretion by primary human
193 colonoids. In addition, the results shown that in addition to BFT, other factors in OMVs inhibit
194 CFTR Cl^- secretion.

195 Twenty-four hours after a 1 hour exposure to OMVs, neither OMVs secreted by ETBF, ETBF
196 Δ*bft* or NTBF reduced CFTR Cl^- secretion compared to PC (**Figure 5**). However, 24 hours after
197 exposure NTBF+ *bft* OMVs reduced CFTR Cl^- secretion (P=0.00364) compared to NTBF OMVs
198 (**Figure 5**). Thus, NTBF+*bft* OMVs have a long term effect (24 hrs.) to inhibit CFTR Cl^-
199 secretion, as opposed to the other OMVs.

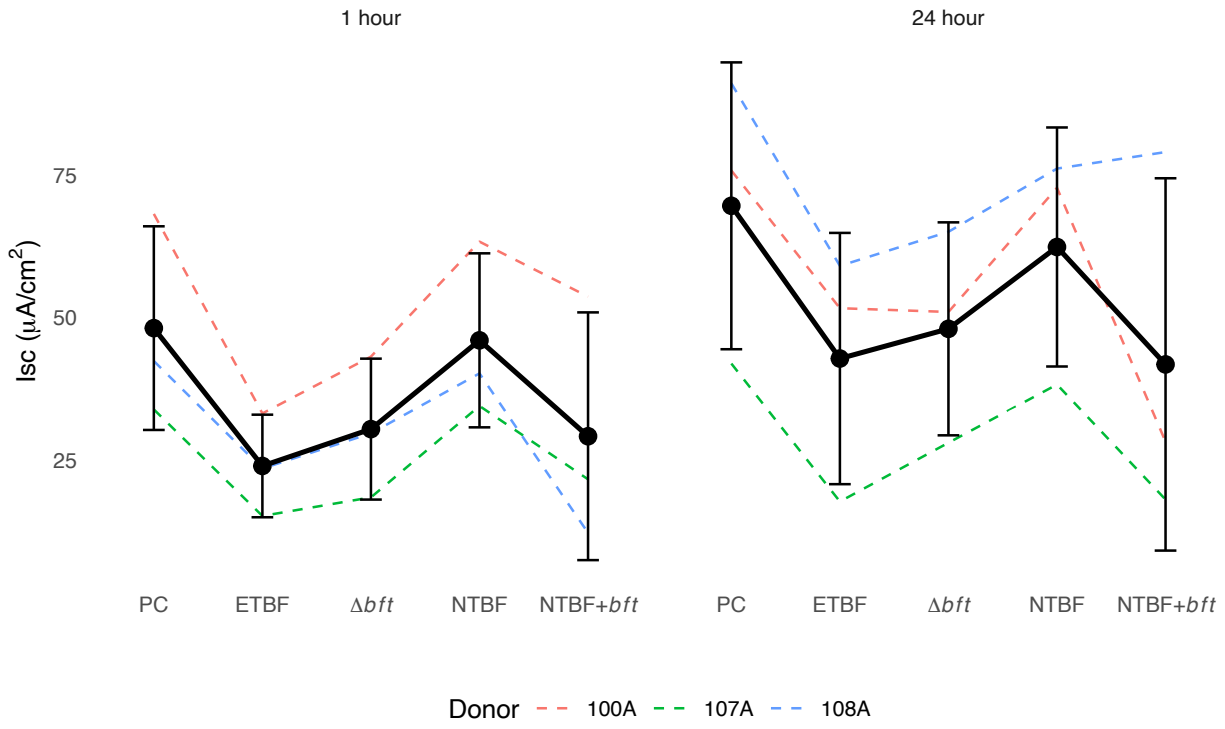

200

201 **Figure 5. CFTR Cl^- secretion by human primary colon organoids.** Left: 1 hour after
202 exposure to PC or OMVs. Right: 24 hours after a 1 hour exposure to PC or OMVs. Individual
203 donor responses are shown as dashed colored lines, with each color representing a different
204 donor (n = 3 donors; Donor 108A is female, Donors 100A and 107A are male). Solid black lines
205 connect the mean current values across treatments. Error bars represent ± 1 standard deviation
206 of measurements. Treatments: PC (process control), ETBF (Enterotoxigenic *B. fragilis*), Δ*bft*
207 (ETBF mutant lacking *bft*), NTBF (Non-toxigenic *B. fragilis*), and NTBF+*bft* (NTBF strain
208 complemented with *bft*). Statistical analysis was performed using mixed-effects linear models
209 with donor as a random effect for each time point separately. Many significant differences from
210 PC were observed at 1 h (ETBF, P = 0.000; Δ*bft*, P = 0.000; NTBF, P = 0.262; NTBF+*bft*, P =
211 0.003). Fewer differences from PC were observed at 24 h compared to PC (ETBF, P =
212 0.693; Δ*bft*, P = 0.244; NTBF, P = 0.525; NTBF+*bft*, P = 0.008). Expression of *bft* in NTBF
213 OMVs reduced the Isc at 1 hour (P = 0.012) and 24 hours (P = 0.004) compared to NTBF

214 OMVs. Experiments were done with three technical replicates per donor of colon cells and three
215 technical replicates of OMVs on three donors.

216

217 Studies were also conducted to determine if OMVs had an effect on transepithelial resistance
218 (TER), since previous studies have shown that recombinant BFT reduced TER in several cell
219 lines [9,13,15-17]. However, none of the OMVs had a significant effect on TER (**Figure 6**) compared
220 to process control (PC) at 1 hour after exposure to OMVs or 24 hours after a 1 hour exposure.

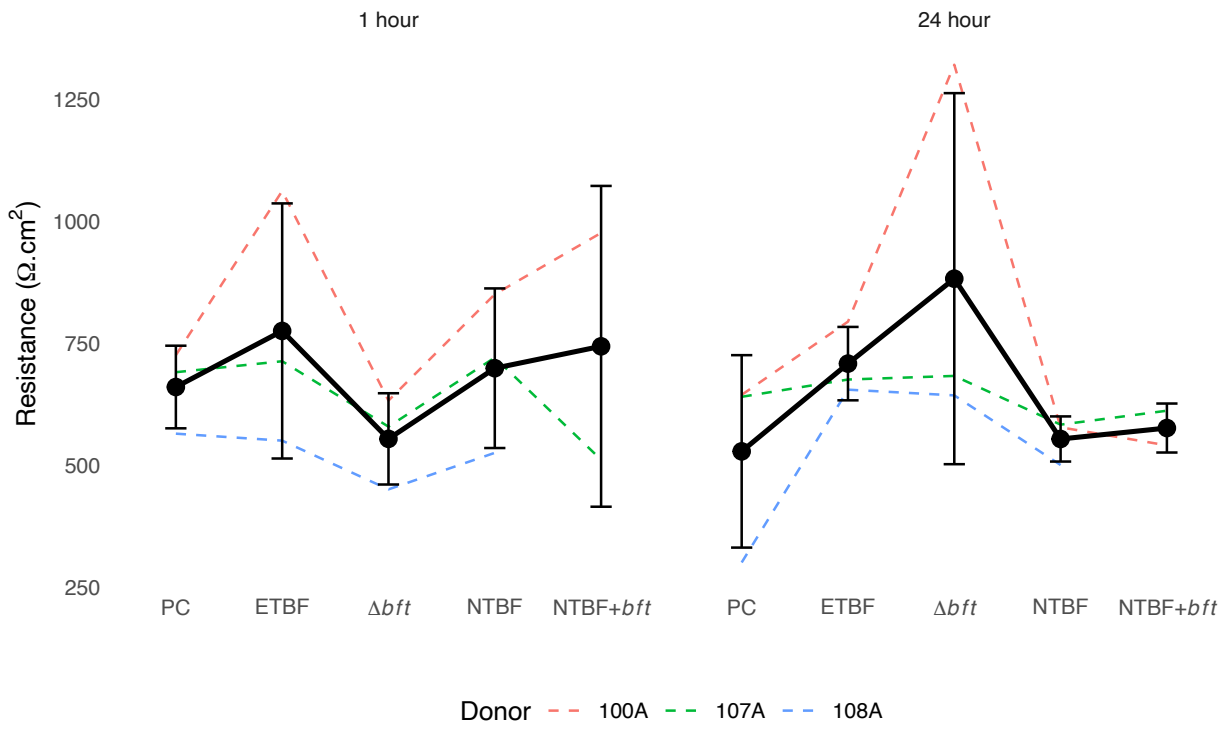

221

222 **Figure 6. Transepithelial resistance (TER) of primary human colonoids**. TER was
223 measured in colon organoids in which CFTR Cl^- secretion was measured 1 hour (left figure) or
224 24 hours (right figure) after exposure to process control (PC) or OMVs secreted by ETBF, ETBF
225 Δ*bft*, NTBF and NTBF+*bft*. Experiments done with three donors, three technical replicates per
226 donor and three technical replicates of OMVs. Technical replicates averaged as a single data

227 point. Individual donor responses are shown as dashed colored lines, with each color
228 representing a different donor (Donor 108A is female). Solid black lines connect the mean
229 resistance values across treatments. Error bars represent ± 1 standard deviation. Statistical
230 analysis was performed using a mixed-effects linear model with donor as a random effect. No
231 significant differences compared to PC (1 and 24 hour exposure) were observed (P>0.05).

232

233 **Bacteroides reduces CFTR Cl^- secretion by T84 cells but has no effect on TER.** We
234 conducted additional studies on T84 cells, a cell line that is used to study the colon [36-38].
235 Previous studies have shown that recombinant BFT reduces the TER [9,13,15-17]. To determine if *B.*
236 *fragilis* OMVs also reduced CFTR Cl^- secretion by T84 cells we conducted Ussing experiments
237 on monolayers of T84 cells under conditions identical to exposure of PC and OMVs to primary
238 colonoids (**Figure 7**). Compared to PC, CFTR Cl^- secretion was reduced by all OMVs (Figure 7,
239 P = 0.001). ETBF OMVs were not more effective than NTBF OMVs in reducing CFTR Cl^-
240 secretion (P = 0.2038). Moreover, deletion of *bft* in ETBF did not significantly reduce the effect
241 of ETBF OMVs on CFTR Cl^- secretion. Thus, there is a notable difference in the response of
242 primary colonids and T84 cells to OMVs. OMVs also had no effect on TER (**Figure 7**). Thus,
243 OMVs reduced CFTR Cl^- secretion by both primary human colonocytes and T84 cells, without
244 altering TER.

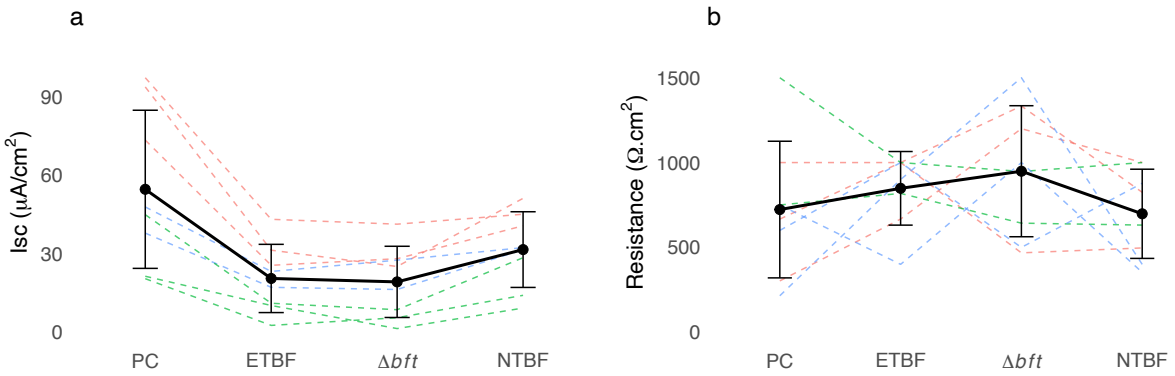

245

246 **Figure 7. CFTR Cl^- secretion and TER by T84 cells exposed to OMVs.** The protocol was
247 identical to that performed on primary human colonoids. T84 monolayers were exposed to outer
248 membrane vesicles from various *B. fragilis* strains for 1 hour and CFTR Cl^- secretion (short-
249 circuit current: Isc) was measured. Data represent individual experiments (dashed lines)
250 grouped by experimental date (colors) with overall means ± standard deviation (black bars with
251 error bars). PC, process control; ETBF, Enterotoxigenic *B. fragilis*; Δbft, ETBF strain with the *bft*
252 gene deletion; NTBF, non-toxigenic *B. fragilis*. n = 8 independent experiments conducted on 3
253 different days. (A) CFTR Cl^- secretion. Each line connects experiments conducted on the same
254 day on the same pass of T84 cells. (B) Transepithelial resistance in the same set of T84 cells
255 used for measurements of CFTR Cl^- secretion. No significant differences in TER from PC were
256 observed after 1 h of exposure to OMVs (ETBF, P = 0.579472; Δbft, P = 0.312689; NTBF, P=
257 0.717002).

258

259 **OMVs do not alter tight junction or cell adhesion protein abundance.** Previous studies
260 have shown that recombinant BFT rapidly (<1 hr.) reduces the expression of the cell adhesion
261 protein E-cadherin in cell lines [9,13,15-17]. However, we observed no effect of Bacteroides OMVs
262 on the abundance of E-cadherin as determined by immunofluorescence microscopy or on the
263 tight junction protein claudin 2 [39,40] (**Figure 8**).

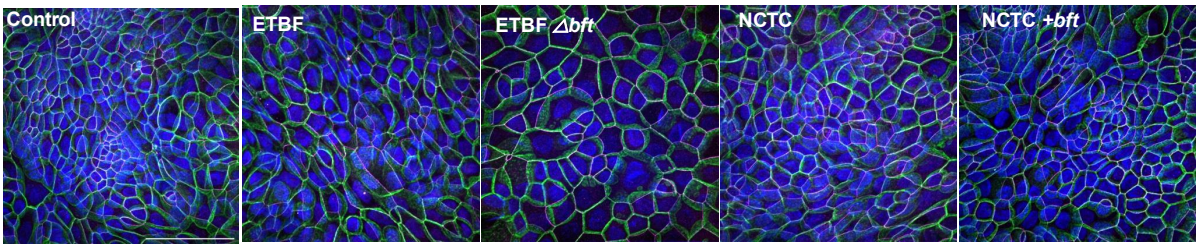

264

265 **Figure 8. Representative composite images of colon organoids.** Organoids were grown on
266 Transwell filters and exposed to OMVs for 1 hour. Claudin-2 (magenta) and E-cadherin (green)
267 were identified by immunofluorescence. DAPI (blue) identified nuclei. Each image is a
268 composite of colonoids labeled for claudin-2, E-cadherin and nuclei (DAPI). Confocal images
269 were analyzed by an investigator (Zdenek Svindrych, Ph.D. Microscopy Imaging Specialist,
270 Dartmouth College) who was blinded to the treatment. There was no difference in claudin-2 or
271 E-cadherin abundance using Fiji open-source image processing package to quantify
272 fluorescence intensity (see **Figure 9** for data).

273

274 As described in Methods, studies were also conducted to measure E-cadherin and claudin-2
275 fluorescence imaged by confocal microscopy. None of the OMVs had any effect on E-cadherin
276 or claudin fluorescence (**Figure 9**) confirming the immunofluorescent images in Figure 8.

277

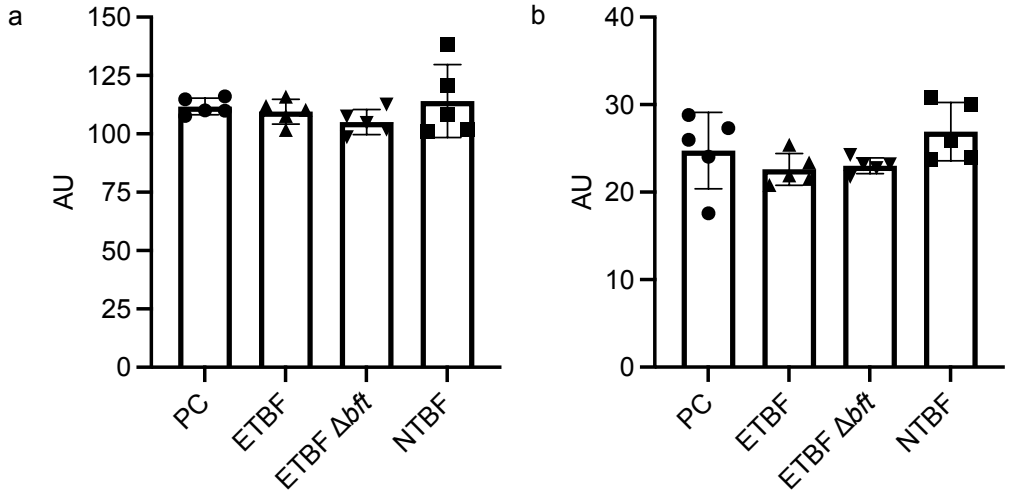

278

279 **Figure 9. Measurements of E-cadherin (a) and claudin (b) epifluorescence**. Data were
280 generated by a co-author blinded to the experimental treatment. Five random images were

281 chosen for each treatment. There was no significant effect of any OMVs on E-cadherin or
282 claudin abundance. AU, arbitrary fluorescent units. Data expressed as mean ± one SD.

283

284 **Cytokine secretion by human primary colonoids.**

285 Previous studies on cell lines and human colon tissue reported that *B fragilis* and recombinant
286 BFT stimulates IL-8 secretion [9,13,15-17,41]. To examine the effect of OMVs on the colon innate
287 immune response, colon organoids were grown on Transwell filters and exposed to PC or
288 OMVs in the apical media for 1 hour or 24 hours after OMVs were removed by washing. **Figure**
289 **10** demonstrates that OMVs had no significant effect on IL-8 secretion compared to PC.
290 Moreover, there was no significant effect of any OMVs compared to PC on the secretion of 48
291 cytokines measured using the MILLIPLEX MAP Human Cytokine/Chemokine 48-Plex cytokine
292 assay, although there were some trends in the response. For example, compared to PC, ETBF
293 OMVs tended to reduce cytokine secretion, although the changes were not significant.

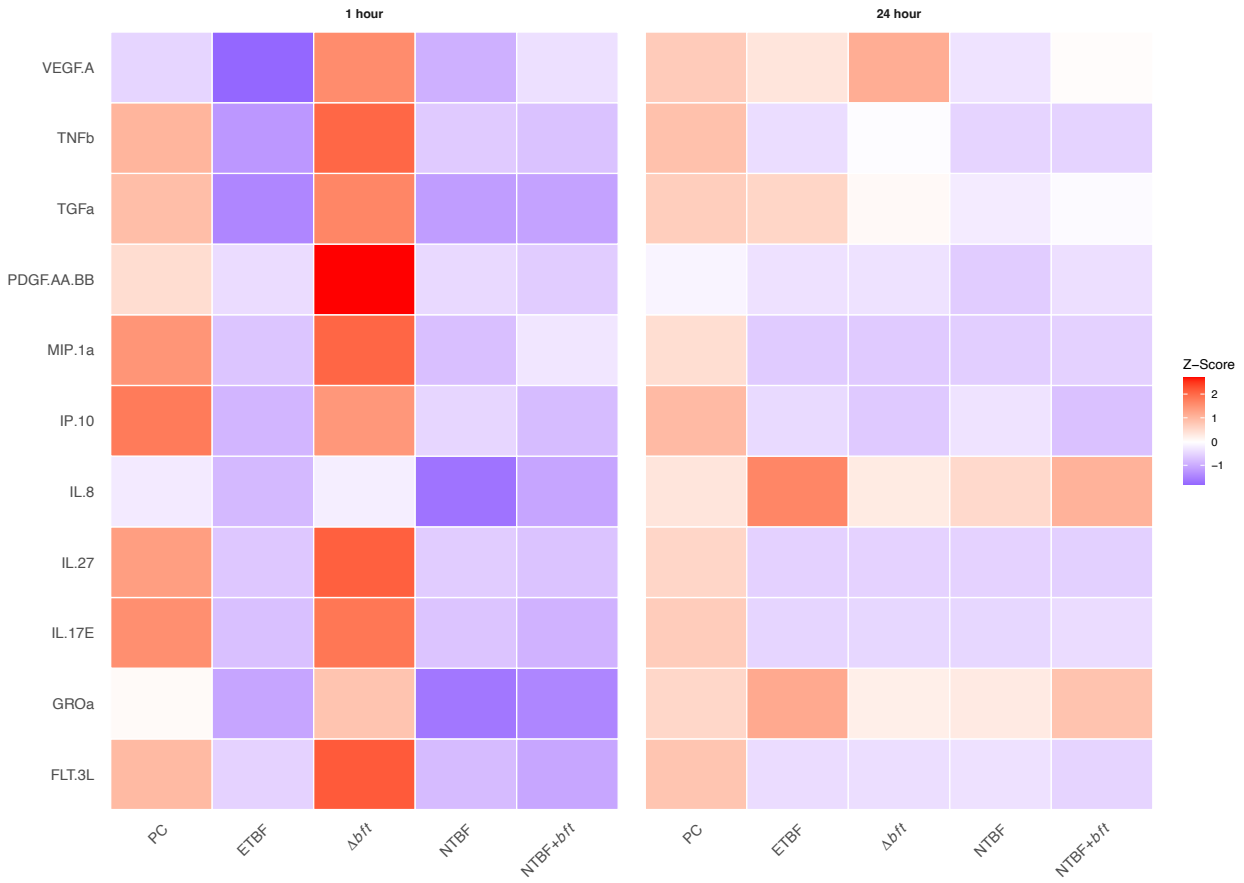

Figure 10. Cytokine secretion following 1 h and 24 hrs. after exposure to OMVs secreted by *B. fragilis* or to PC. There were no significant effects of OMVs versus PC. Values represent means across all donors (n = 3 donors, including one female) for each treatment condition. Treatments: PC, ETBF, ETBF Δ*bft*, NTBF and NTBF+*bft*. Color scale indicates standard deviations from the time point mean: red represents above-average expression, blue represents below-average expression, and white represents average expression for each cytokine at each time point. Only cytokines with complete data (values above detection) across all conditions are shown. Data were log2-transformed prior to z-score calculation.

Discussion

305 The goal of this study was to elucidate the effect of OMVs secreted by *B. fragilis* on human
306 primary colonoids. To this end we developed a model to study pathogen-host interactions where
307 we examined the effect of OMVs secreted by several strains of *B. fragilis* on monolayers of well
308 differentiated, primary human colon organoids. We found that OMVs secreted by most strains of
309 Bacteroides reduced CFTR Cl^- secretion compared to PC after 1 hour exposure. Deletion of the
310 *bft* gene from ETBF reduced the inhibitory effect of ETBF OMVs on CFTR Cl^- secretion.
311 Moreover, NTBF+*bft* OMVs were more inhibitory to CFTR Cl^- secretion compared to OMVs
312 secreted by NTBF. Twenty four hours after exposure to OMVs only NTBF+*bft* OMVs reduced
313 CFTR Cl^- secretion compared to NTBF OMVs. Thus, BFT in OMVs was, at least in part,
314 responsible for the decrease in CFTR Cl^- secretion by primary human colonoids. Since OMVs
315 secreted by strains of *B. fragilis* that lacked *bft* also reduced CFTR Cl^- secretion, there must be
316 other factors in OMVs such as proteins or miRNAs, for example, that inhibit forskolin-stimulated
317 CFTR Cl^- secretion, as shown previously for OMVs secreted by *P. aeruginosa* [18-20,42-44].
318 Additional studies are required to identify these factors. Importantly, none of the OMVs tested
319 had any effect on the abundance of the tight junction protein claudin-2, or the cell adhesion
320 protein E-cadherin or on the TER. Claudin-2 is an important component of the tight junction, and
321 alterations in claudin-2 abundance affects TER[39,40]. We conclude that in our studies OMVs have
322 no effect on tight junction or cell adhesion structure but does inhibit CFTR Cl^- secretion by
323 primary proximal human colon organoids developed from biopsies obtained during
324 colonoscopies.

325 Studies were also conducted to examine the effect of *B. fragilis* OMVs on CFTR Cl^- secretion
326 and TER by the T84 colon cell line. *B. fragilis* OMVs reduced CFTR Cl^- secretion but had no
327 effect on TER. This result was similar to the effect of OMVs on primary human colonoids and
328 was opposite to what was observed with recombinant BFT in T84 and other colon cell lines[9,13,15-
329 17]. However, it should be noted that there are some differences between the response of

330 colonoids and T84 cells to OMVs. Most significantly, in T84 cells deletion of *bft* from OMVs
331 secreted by ETBF had no effect on CFTR Cl^- secretion (ETBF versus ETBF Δbft: Figure 7A).

332 There are a few other reports describing the development of monolayers of epithelial cells
333 derived from healthy colon organoids [29,30]. Sen et al. [30] reported that the gene expression profile
334 of human colon organoids was significantly different from the Caco-2 cell line, an immortalized
335 cell line of human colorectal adenocarcinoma cells, which had a gene expression profile similar
336 to the small intestine. Moreover, they reported that the effect of *Bifidobacterium longum* on gene
337 expression was not conserved between Caco-2 and colon organoids. Taglieri et al [29] reviewed
338 the literature on human colon monolayers and noted that air liquid interface culture, like that
339 used in the present study, increased differentiation of colon monolayers. However, none of the
340 other studies on colon monolayers exposed them to OMVs and none reported CFTR Cl^-
341 secretion.

342 OMVs secreted by most strains of *B. fragilis* inhibited forskolin-stimulated CFTR Cl^- secretion by
343 the proximal colon and T84 cells, which would reduce salt and fluid secretion by the colon.
344 However, studies in animals report that recombinant BFT induces secretory diarrhea [3,6-8]. One
345 possible reason for the different effects of recombinant BFT and OMVs containing BFT is that
346 the effect of recombinant BFT may be dose dependent, and that recombinant BFT levels in
347 published studies may be higher than the abundance of BFT in OMVs. Moreover, as
348 demonstrated in Figures 5 and 7 and the Supplemental Tables, OMVs contain many proteins in
349 addition to BFT, that are likely to inhibit CFTR Cl^- secretion. Finally, it is important to note that
350 there are other pathways that mediate transepithelial salt and water transport by the proximal
351 colon, including electroneutral NaCl and fluid reabsorption mediated by the parallel operation of
352 Na^+/H^+ and Cl^-/HCO_3^- (SLC26A3) exchangers. Since Ussing chamber studies only measure
353 electrogenic transport, it is possible that recombinant BFT may inhibit SLC26A3 and/or the
354 Na^+/H^+ exchanger and thereby reduce electroneutral NaCl and fluid reabsorption by the colon.

355 Such an effect may account for the BFT-induced secretory diarrhea, despite the OMV and BFT
356 reduction in electrogenic CFTR Cl^- secretion reported herein. Thus, additional studies, beyond
357 the goals of the present study, are required to determine if BFT and OMVs inhibit Na^+/H^+ and Cl^-
358 $/HCO_3^-$ electrically neutral NaCl and fluid reabsorption in primary human colonoids.

359 We also did not observe an effect of any OMVs on the TER or epithelial tight junction or cell
360 adhesion structure. In many, but not all, previous studies in colon cell lines recombinant BFT
361 quickly (< 1 hr.) reduced the abundance of E-cadherin and the transepithelial resistance [9,13,15-17].
362 Although the reason for this difference is unknown, one possible reason for the different effects
363 of recombinant BFT and OMVs is that, as noted above, the effect of recombinant BFT may be
364 dose dependent, and that recombinant BFT levels in published studies may be higher than the
365 abundance of BFT in OMVs.

366 In contrast to studies using cells lines and recombinant BFT [10,46-48], we did not observe an
367 increase in IL-8 secretion in primary human colonoids exposed to OMVs. The lack of effect of
368 BFT and OMVs on IL-8 secretion in our study are consistent with the observation that OMVs did
369 not reduce E-cadherin, an effect reported to be required for BFT to stimulate IL-8 secretion [10,46-
370 48]. Moreover, OMVs did not affect the secretion of 48 cytokines as determined by the
371 MILLIPLEX MAP Human Cytokine/Chemokine 48-Plex cytokine assay. The reason for this
372 difference requires additional studies.

373 There are a few limitations of our study. First, since there are many differences in the content of
374 OMVs secreted by ETBF and NTBF such as DNA, RNA, miRNA, proteins (this study) and other
375 virulence factors [21,49], in addition to BFT, it is possible that some of these factors may act in
376 concert with BFT or act alone to inhibit CFTR Cl^- secretion. Thus, we cannot rule out the
377 possibility that other factors, such as proteins, DNA or miRNAs, may contribute to the OMV-
378 induced inhibition of CFTR Cl^- secretion. Notably, one other study demonstrated that NTBF

379 secretes OMVs that deliver cargo into Caco-2 cells, and activates Toll-like receptors; however,
380 the study did not report the effect of OMVs on cytokine secretion or CFTR Cl^- secretion [50].

381 Our study has numerous strengths. First, our experiments were conducted on primany human
382 colonoids from several healthy donors, and a cell line (T84). OMVs inhibited CFTR Cl^- secretion
383 by colonoids and T84 cells, but had no effect on TER. Second since *B. fragilis* resides in mucus
384 overlying colon cells, OMVs containing BFT are biologically relevant. Notably, the concentration
385 of OMVs used in the present study was similar to levels observed in conditioned cell culture
386 media and biological fluids [18,51]. Third, we confirmed the presence of BFT in ETBF OMVs and its
387 absence in NTBF OMVs by proteomic analysis and the absence of *bft* in NTBF and ETBF Δ*bft*
388 and the presence of *bft* in NTBF+*btf* by qPCR.

389 In conclusion, we have examined the effect of OMVs on well differentiated primary cultures of
390 human proximal colon using strains of *B. fragilis* containing *bft (*ETBF and NTBF+*bft)*, a strain of
391 *B. fragilis* in which *bft* was knocked out (ETBF Δ*bft*), and an NTBF strain that does not express
392 *bft.* In all cases BFT containing OMVs secreted by *B. fragilis* reduced forskolin-stimulated CFTR
393 Cl^- secretion more than the same strain lacking *bft*, but had no effect on tight junction structure,
394 TER or IL-8 secretion. Similar experiments on the T84 cell line also revealed that OMVs
395 secreted by *B. fragilis* reduced CFTR Cl^- secretion and had no effect on TER. We conclude that
396 *B. fragilis* OMVs inhibit forskolin stimulated CFTR Cl^- secretion by primary human colonoids.
397 Thus, OMVs are an important mechanism of host pathogen interactions in the proximal colon.
398 Additional studies, beyond the scope of the present study, are required to elucidate the cellular
399 mechanisms whereby OMVs rapidly inhibit CFTR Cl^- secretion.

400 **METHODS**

401 **Bacteroides cultures**. *B. fragilis* NCTC 9343 was chosen as the non-toxigenic *B. fragilis*
402 (NTBF) strain, since it is used widely [52-54]. *B. fragilis* 86-5443-2-2 was chosen as the

403 enterotoxigenic *B. fragilis* (ETBF) strain for similar reasons, and because it expresses BFT-2,
404 which is the most virulent of the three BFT isotypes [52-54]. *B. fragilis* 86-5443-2-2 with a *bft*
405 deletion (ETBF Δ*bft*) and NTBF+*bft* were confirmed by PCR. Bacteroides strains were grown on
406 supplemented brain heart infusion medium (BHIS) agar plates or liquid broth cultures
407 supplemented with hemin and 1μg/ml of vitamin K3 (Acros Organics/Fisher Scientific, Geel,
408 Belgium) under anaerobic conditions (10% CO_2, 10% H_2, 80% N_2) in a Whitley A55 anaerobic
409 chamber (Don Whitley Scientific, Victoria Works, UK) at 37°C. All BHIS agar and liquid media
410 contained 60 μg/ml of gentamycin sulfate. For OMV purification, *B. fragilis* strains were streaked
411 on BHIS agar plates and were grown in anaerobic conditions for 48 hours. Single colonies were
412 used to inoculate 5mL of BHIS liquid medium cultures, which were grown anaerobically for 24
413 hours. The cultures were then expanded into 200mL BHIS cultures using a 1:100 dilution. The
414 final cultures were grown for 24 hours prior to being utilized to isolate OMVs.

415 **Outer membrane vesicle (OMV) isolation.** OMVs were isolated as described by us and others
416 previously [20,55]. Briefly, all overnight culture supernatants were centrifuged for 1 h at 2800 g and
417 4°C to pellet bacteria. The supernatant was filtered twice through 0.45 μm PVDF membrane
418 filters (Millipore, Billerica, MA, USA) to remove any contaminating bacteria and concentrated
419 with 30K Amicon filters (Millipore, Billerica, MA, USA) at 2800 g and 4°C to obtain ~200 μL of
420 concentrate. The concentrate was resuspended in OMV buffer (20 mM HEPES, 500 mM NaCl,
421 pH 7.4) and subjected to ultracentrifugation using a TH-660 Swinging Bucket rotor (Thermo
422 Fisher) for 2 h at 200,000 g and 4°C to pellet OMVs. OMV pellets were then re-suspended in
423 60% OptiPrep Density Gradient Medium (Sigma-Aldrich, Cat. # D1556) and layered with 40%,
424 35%, 30% and 20% OptiPrep diluted in OMV buffer. OMVs in OptiPrep were centrifuged for 16
425 h at 100,000 g and 4°C. 500 μl fractions were taken from the top of the gradient, with OMVs
426 residing in fractions 5-8, as determined by proteomic analysis of OMVs.

427 **Electron microscopy of OMVs**. OMVs were visualized with negative staining transmission
428 electron microscopy as described previously [19]. Briefly, an aliquot of each sample was applied
429 onto a freshly glow-discharged 200-mesh nickel grid and allowed to sit for two minutes. After
430 incubation, excess fluid was gently removed with filter paper, and the grids were sequentially
431 rinsed with Millipore-filtered distilled water. While the grids remained slightly damp, they were
432 placed onto a drop of Nano-W tungsten stain (Ted Pella, Inc.). Excess stain was absorbed with
433 filter paper, and the staining step was repeated on a second drop of Nano-W, which was
434 allowed to sit for one minute before being wicked away and left to dry. Imaging of the stained
435 grids was conducted at 80 kV on a JEOL 1400 transmission electron microscope (JEOL USA
436 Inc.), and images were captured using an AMT XR11 digital camera (AMT). The imaging of
437 OMVs were conducted by an investigator blinded to the sample identities.

438 **Proteomics characterization of OMVs.** To confirm that BFT was secreted by ETBF in OMVs,
439 but not by NTBF, OMVs from ETBF and NTBF were isolated as described above and pelleted
440 and flash-frozen in liquid nitrogen for proteomic analysis. Mass spectrometry analysis was
441 performed by the Mass Spectrometry Technology Access Center (MTAC) at Washington
442 University School of Medicine using a previously published protocols [56]. Briefly, we used 52 µg
443 of protein per sample for purification via TCA precipitation. The proteins were reduced,
444 alkylated, and digested with trypsin. Digested peptides were desalted on C18 columns and then
445 peptide quantification was measured by nanodrop assay. An equal amount of each sample was
446 subject to mass spec analysis by randomization. All samples were analyzed in technical
447 duplicates by liquid chromatography-tandem mass spectrometry (LC-MS/MS) using a Neo trap
448 cartridge coupled with an analytical column (75 µm ID x 50 cm PepMapTM Neo C18, 2 µm).
449 Samples were separated using a linear gradient of solvent A (0.1% formic acid in water) and
450 solvent B (0.1% formic acid in ACN) over 120 minutes using a Vanquish Neo UHPLC System
451 coupled to an Orbitrap Eclipse Tribrid Mass Spectrometer with FAIMS Pro Duo interface

452 (Thermo Fisher Scientific). Protein tandem MS data was queried for protein identification and
453 label-free quantification against a *B. fragilis* database (National Center for Biotechnology
454 Information) using MaxQuant. The following modifications were set as search parameters:
455 trypsin digestion cleavage after K or R (except when followed by P), 2 allowed missed cleavage
456 site, carbamidomethylated cysteine (static modification), and oxidized methionine, protein N-
457 term acetylation (variable modification). Search results were validated with peptide and protein
458 FDR both at a p value <0.01. Proteins that were identified with >1 unique peptide were
459 subjected to a downstream statistical analysis.

460 Resulting data was aligned to associated protein files for NTBF or ETBF for protein
461 identification. Using .faa files for these strains obtained from the National Center for
462 Biotechnology Information, we determined which proteins are common and unique between the
463 two strains by merging their accession numbers. Each common protein file was then used to
464 filter the proteomics results of both strains prior to differential expression analysis between the
465 two strains. R v.4.3.0 and DESeq2 v.1.40.2 were used for differential analysis, using NTBF as
466 the control strain and ETBF as the treatment strain. P values were adjusted for multiple
467 comparisons using the Benjamini-Hochberg correction. Differentially expressed proteins that
468 had an adjusted p-value < 0.05 were used for hierarchal clustering.

469 **Colonoid cell culture.** Biopsies from the proximal colon obtained during colonoscopies of three
470 healthy de-identified donors were obtained after informed consent at Dartmouth-Hitchcock
471 Medical Center. Biopsies in PBS (-/-) with EDTA were placed on a shaking rocker in +4°C for 1
472 hour to free the crypts from the biopsies. Then the biopsies were vigorously pipetted up and
473 down several times to release crypts. The supernatant containing crypts was collected, and
474 additional PBS was added to the biopsies followed by vigorous pipetting. Crypts in the
475 supernatant were counted, pelleted, and resuspended in 55% Matrigel (Corning Life Sciences)
476 and 45% isolation medium. Cells were added to 24-well plates and then Matrigel solidified cell

477 isolation medium (IntestiCult complete medium with primocin [StemCell Technologies]
478 supplemented with 50ug/mL gentamycin, 50ug/mL vancomycin and 10uM of RhoKi) was added
479 to each well. Cells were maintained in culture until 3D organoids were observed. To develop
480 polarized monolayers of organoids, $1.5x10^6$ cells (as 3D organoids) were collected from the
481 Matrigel and seeded on Transwell permeable filters (#3450: Corning Life Sciences for 24-mm
482 Transwell) or 12-mm Snapwell permeable filters (#3801; Corning Life Sciences). Filters were
483 precoated with 1:20 dilution of matrigel in cold DPBS for 2 hours and then removed just before
484 seeding cells. IntestiCult media (StemCell Technologies) was added to both apical and
485 basolateral sides of the filters to support cell growth. Once a confluent monolayer was obtained,
486 IntestiCult differentiation media (StemCell Technologies) was used to differentiate the cells prior
487 to experimentation. Cells were differentiated for one week before experiments.

488 **Exposure of primary human colonids to OMVs.** Polarized monolayers of colon cells on 12-
489 mm Snapwell filters were washed with PBS to remove excess mucus, and 1.5 mL of
490 differentiation media was added to the basolateral side. 2×10^{10} OMVs, a concentration of OMVs
491 lower than measured in conditioned media and in biological fluids [18,51], or the same volume of
492 process control media were applied to the apical side of cells for one hour and then removed by
493 washing in PBS. At the end of the one-hour exposure and then twenty-four hours later the apical
494 and basolateral media were collected for measurements of cytokines [MILLIPLEX MAP Human
495 Cytokine/Chemokine 48-Plex cytokine assay (MilliporeSigma)]. Ussing chamber analysis was
496 used to quantify CFTR Cl^- secretion and TER.

497 **T84 cell culture**. T84 cells, a human colon adenocarcinoma cell line (American Type Culture
498 Collection, Manassas, VA) were maintained in DMEM/F-12 media (Life Technology, Rockville,
499 MD) containing l-glutamine supplemented with 5% fetal bovine serum (FBS: Life Technology).
500 For short-circuit current and TER measurements cells were cultured on Transwell filters

501 (Corning, Ithaca, NY). Experiments were performed 14 days postseeding as previously
502 described [36-38].

503 **Ussing chamber measurements of CFTR Cl^- currents.** As described in detail elsewhere [57-60]
504 cells on Transwell filters were mounted in Ussing chambers. Primary human colon organoids
505 and T84 cells were exposed to either process control (PC: BHIS growth media processed
506 through the OMV isolation procedure, as a control for possible effects on colon monolayers due
507 to the media or the OMV isolation process as recommended by the International Society of
508 Extracellular Vesicles [61]) or OMVs secreted by ETBF, ETBF Δ*bft*, NTBF, or NTBF+*bft* were
509 added to the apical side of monolayers for 1 hour then CFTR Cl^- currents and TER were
510 measured. Some monolayers were exposed to OMVs for 1 hour, followed by washing OMVs
511 from the apical surface and 24 hours later CFTR Cl^- currents and TER were measured. To
512 measure TER, a 1 mV pulse was applied to each monolayer and the change in short circuit
513 current was measured and TER was calculated using Ohms Law. To measure forskolin-
514 stimulated CFTR Cl^- secretion, amiloride (50 μM) was first added to the apical solution to inhibit
515 potential electrogenic Na^+ reabsorption. Thereafter, Cl^- secretion was stimulated with forskolin
516 (10 μM; Sigma-Aldrich). Finally, thiazolidinone ($CFTR_{inh}$-172, 20 μM; Millipore, Billerica, MA), an
517 inhibitor of CFTR Cl^- channels, was added to the apical solution [58]. Data are expressed as the
518 forskolin-stimulated, $CFTR_{inh}$-172 inhibited short circuit current (Isc), which is presented as
519 $\mu A/cm^2$. Data were collected and analyzed using the Data Acquisition Software Acquire and
520 Analyze program (Physiologic Instruments, San Diego, CA).

521 **Cytokine measurements.** Cytokine secretion (apical and basolateral solutions) from primary
522 colonoids was measured with the MILLIPLEX MAP Human Cytokine/Chemokine 48-Plex
523 cytokine assay (MilliporeSigma) following the manufactures instructions

524 **Immunocytochemistry.** Immunocytochemistry was performed to characterize cell types in the
525 colon monolayers and to evaluate the effects of OMVs on E-cadherin and claudin. Fixation of
526 monolayers of colonoids was performed using 4% paraformaldehyde for 15 minutes at room
527 temperature, followed by permeabilization with 0.25% Triton X-100 for 15 minutes, blocking
528 using 10% normal goat serum in PBS, and primary antibody incubation at 4°C overnight. After
529 washing, secondary antibodies were added for 1 hour at room temperature in the dark.
530 SLC26A3 was labeled with a primary anti-mouse antibody (1:250, Santa Cruz #sc-376187), and
531 a secondary goat anti-mouse-488 antibody (1:500, Santa Cruz #sc-376187). CFTR was labeled
532 with a primary anti-mouse antibody (1:100, Millipore # 05-583) and a secondary anti-mouse-488
533 antibody (1:500). MUC2 was labeled with a primary anti-mouse antibody (1:300), and a
534 secondary anti-mouse-488 antibody (1:500, Abcam ab11197). Chromogranin A was labeled
535 with a primary goat anti rabbit antibody (1:100), and secondary goat anti rabbit-568 antibody
536 (1:1000, Abcam ab15760). Tight junction labeling was performed by fixing cells in 100% cold
537 methanol at -20°C for 5 minutes, blocking with 10% goat serum in PBS for one hour, and
538 incubating with primary antibodies at 4°C overnight. The secondary antibody was added for 1
539 hour at room temperature the following day. Claudin-2 was labeled using a primary goat anti-
540 rabbit antibody (1:100, Thermo Fisher #51-6100), and a secondary goat anti-rabbit-568 antibody
541 (1:500). E-cadherin was labeled using a primary goat anti-mouse antibody (1:250, BD
542 Transduction lab #610182), and a secondary goat anti-mouse-488 antibody (1:500). All
543 antibodies were diluted in PBS with 5% normal goat serum. DAPI staining to label nuclei was
544 performed in fluorshield anti-fade mounting medium. To image the colon monolayers, a Nikon
545 Eclipse Ti-E spinning disc confocal microscope was used. To examine the effect of OMVs and
546 PC on claudin-2 and E-cadherin, all settings on the confocal microscope were identical for
547 acquiring images for analysis. Analysis of claudin-2 and E-cadherin abundance was performed
548 by an investigator blinded to the treatments. The membrane areas with positive fluorescence
549 signal were segmented using trainable WEKA machine learning plugin in ImageJ [62]. The

550 segmented objects were thinned to 1 pixel using ImageJ's "Skeletonize" morphological
551 operation. The mean and median fluorescence intensities were measured from areas defined by
552 the skeleton, and widened to 5 pixels using ImageJ's "Dilate" morphological operation.

553 **Statistics.** Data were analyzed using the R software environment for statistical computing and
554 graphics version 4.1.0 [63] and Ingenuity Pathway Analysis. Statistical significance was calculated
555 using either a mixed effect linear model, or likelihood ratio tests on gene-wise negative binomial
556 generalized linear models, as indicated in the figure legends. Data were visualized, and figures
557 were created using the R package ggplot2 [64].

558 **Author contributions**

559 PS, RB, AN, BAS, CR, TTH and BR designed the research studies. PS, RB, AN, CR, TTH and
560 ZS conducted experiments on colon organoids, acquired data, and analyzed data. TBG
561 recruited human subjects, provided informed consent and collected clinical biopsies. YAG and
562 BKC performed the proteomics analysis of OMVs. Electron microscopy of OMVs was performed
563 by DJT at the Microscopy Imaging Center at the University of Vermont (RRID# SCR_018821).
564 BAS wrote the manuscript. All authors contributed to the article and approved the submitted
565 version.

566 **Declaration of competing interests**

567 All authors declare no competing interests.

568 **IRB statement**

569 The Dartmouth Committee for the Protection of Human Subjects has determined that using colon
570 biopsies in this study is not considered human subject research because they contain no patient
571 identifiers. All tissues used for isolation were obtained under informed consent and conform to
572 HIPAA regulations to protect the privacy of the donor's personally identifiable information .

573 **Data availability.** Proteomics data from OMVs are available in the Supplemental Tables. All
574 other reasonable requests for additional data are available from the corresponding author.

575 **Funding Declaration**. This study was supported by the Cystic Fibrosis Foundation
576 (STANTO19G0, STANTO20P0, STANTO23R0, and STANTO19R0) and the National Institutes
577 of Health [P30-DK117469 (Pilot Project Award) and R01HL151385] to BAS. BDR was
578 supported by NIH R35GM142685 and CFF ROSS20R3 and is the Phil Hanlon First Century
579 Associate Professor in Personalized Treatment for Cystic Fibrosis. PS was supported by T32-
580 HL134598. Electron Microscopy was performed at the Microscopy Imaging Center, Larner
581 College of Medicine, University of Vermont (RRID# SCR_01882). Mass Spectrometry analyses
582 were performed by the Mass Spectrometry Technology Access Center at the McDonnell
583 Genome Institute (MTAC@MGI) at Washington University School of Medicine, supported by the
584 Diabetes Research Center/NIH grant P30 DK020579, Institute of Clinical and Translational
585 Sciences/NCATS CTSA award UL1 TR002345, and Siteman Cancer Center/NCI CCSG grant
586 P30 CA091842.

587 **Acknowledgements.** Cynthia Sears, M.D. (Johns Hopkins University) generously provided all
588 ETBF strains. Scott Palisoul (Dartmouth Pathology Shared Resources) created frozen cross
589 sections of 2D colon monolayers. We thank Katja Koeppen, Ph.D. for analysis of the T84 data.

590 **SUPPLEMENTAL TABLES**

591 **Supplemental Table 1.** Mass spectrometry quantification of proteins detected exclusively in *B.*
592 *fragilis* NTBF OMVs.

593 **Supplemental Table 2.** Mass spectrometry quantification of proteins detected exclusively in *B.*
594 *fragilis* ETBF OMVs.

595 **Supplemental Table 3.** Mass spectrometry quantification of proteins detected in both *B. fragilis*
596 NTBF and *B. fragilis* ETBF OMVs.

597 **Supplemental Table 4.** Differential expression results of proteins identified in mass
598 spectrometry for both *B. fragilis* ETBF and *B. fragilis* NTBF

599 **References**

600 1 Jasemi, S. *et al.* Biological Mechanisms of Enterotoxigenic Bacteroides fragilis Toxin:
601 Linking Inflammation, Colorectal Cancer, and Clinical Implications. *Toxins (Basel)* **17**
602 (2025). https://doi.org/10.3390/toxins17060305
603 2 Ferranti, E. P., Dunbar, S. B., Dunlop, A. L. & Corwin, E. J. 20 things you didn't know
604 about the human gut microbiome. *J Cardiovasc Nurs* **29**, 479-481 (2014).
605 https://doi.org/10.1097/JCN.0000000000000166
606 3 Valguarnera, E. & Wardenburg, J. B. Good Gone Bad: One Toxin Away From Disease
607 for Bacteroides fragilis. *J Mol Biol* **432**, 765-785 (2020).
608 https://doi.org/10.1016/j.jmb.2019.12.003
609 4 Human Microbiome Project, C. Structure, function and diversity of the healthy human
610 microbiome. *Nature* **486**, 207-214 (2012). https://doi.org/10.1038/nature11234
611 5 Young, V. B. The role of the microbiome in human health and disease: an introduction
612 for clinicians. *BMJ* **356**, j831 (2017). https://doi.org/10.1136/bmj.j831
613 6 Saha, K., Zhou, Y. & Turner, J. R. Tight junction regulation, intestinal permeability, and
614 mucosal immunity in gastrointestinal health and disease. *Curr Opin Gastroenterol* **41**,
615 46-53 (2025). https://doi.org/10.1097/MOG.0000000000001066
616 7 Hill, C. A. *et al.* Bacteroides fragilis toxin expression enables lamina propria niche
617 acquisition in the developing mouse gut. *Nat Microbiol* **9**, 85-94 (2024).
618 https://doi.org/10.1038/s41564-023-01559-9
619 8 Sears, C. L. *et al.* Association of enterotoxigenic Bacteroides fragilis infection with
620 inflammatory diarrhea. *Clin Infect Dis* **47**, 797-803 (2008).
621 https://doi.org/10.1086/591130

622 9 Kim, W. S. *et al.* Bacteroides fragilis Toxin Induces Sequential Proteolysis of E-Cadherin
623 and Inflammatory Response in Mouse Intestinal Epithelial Cell Line. *Microorganisms* **13**
624 (2025). https://doi.org/10.3390/microorganisms13040781
625 10 Hwang, S., Gwon, S. Y., Kim, M. S., Lee, S. & Rhee, K. J. Bacteroides fragilis Toxin
626 Induces IL-8 Secretion in HT29/C1 Cells through Disruption of E-cadherin Junctions.
627 *Immune Netw* **13**, 213-217 (2013). https://doi.org/10.4110/in.2013.13.5.213
628 11 Rong, Y. *et al.* Partially differentiated ileal and distal-colonic human F508del-cystic
629 fibrosis-enteroids secrete fluid in response to forskolin and linaclotide. *iScience* **28**,
630 112453 (2025). https://doi.org/10.1016/j.isci.2025.112453
631 12 Negussie, A. B., Dell, A. C., Davis, B. A. & Geibel, J. P. Colonic Fluid and Electrolyte
632 Transport 2022: An Update. *Cells* **11** (2022). https://doi.org/10.3390/cells11101712
633 13 Riegler, M. *et al.* Bacteroides fragilis toxin 2 damages human colonic mucosa in vitro.
634 *Gut* **44**, 504-510 (1999). https://doi.org/10.1136/gut.44.4.504
635 14 Obiso, R. J., Jr., Azghani, A. O. & Wilkins, T. D. The Bacteroides fragilis toxin fragilysin
636 disrupts the paracellular barrier of epithelial cells. *Infect Immun* **65**, 1431-1439 (1997).
637 https://doi.org/10.1128/iai.65.4.1431-1439.1997
638 15 Wu, S., Rhee, K. J., Zhang, M., Franco, A. & Sears, C. L. Bacteroides fragilis toxin
639 stimulates intestinal epithelial cell shedding and gamma-secretase-dependent E-
640 cadherin cleavage. *J Cell Sci* **120**, 1944-1952 (2007). https://doi.org/10.1242/jcs.03455
641 16 Kharlampieva, D. D. *et al.* Purification and characterisation of recombinant Bacteroides
642 fragilis toxin-2. *Biochimie* **95**, 2123-2131 (2013).
643 https://doi.org/10.1016/j.biochi.2013.08.005
644 17 Chambers, F. G. *et al.* Bacteroides fragilis toxin exhibits polar activity on monolayers of
645 human intestinal epithelial cells (T84 cells) in vitro. *Infect Immun* **65**, 3561-3570 (1997).
646 https://doi.org/10.1128/iai.65.9.3561-3570.1997

647 18 Charpentier, L. A. *et al.* Bacterial Outer Membrane Vesicles and Immune Modulation of
648 the Host. *Membranes (Basel)* **13** (2023). https://doi.org/10.3390/membranes13090752
649 19 Li, Z. *et al.* P. aeruginosa tRNA-fMet halves secreted in outer membrane vesicles
650 suppress lung inflammation in cystic fibrosis. *Am J Physiol Lung Cell Mol Physiol* **326**,
651 L574-L588 (2024). https://doi.org/10.1152/ajplung.00018.2024
652 20 Koeppen, K. *et al.* A Novel Mechanism of Host-Pathogen Interaction through sRNA in
653 Bacterial Outer Membrane Vesicles. *PLoS Pathog* **12**, e1005672 (2016).
654 https://doi.org/10.1371/journal.ppat.1005672
655 21 Yang, Y. *et al.* Bacteroides Fragilis-Derived Outer Membrane Vesicles Deliver MiR-5119
656 and Alleviate Colitis by Targeting PD-L1 to Inhibit GSDMD-Mediated Neutrophil
657 Extracellular Trap Formation. *Adv Sci (Weinh)*, e00781 (2025).
658 https://doi.org/10.1002/advs.202500781
659 22 Shagaleeva, O. Y. *et al.* Bacteroides vesicles promote functional alterations in the gut
660 microbiota composition. *Microbiol Spectr* **12**, e0063624 (2024).
661 https://doi.org/10.1128/spectrum.00636-24
662 23 Patrick, S., McKenna, J. P., O'Hagan, S. & Dermott, E. A comparison of the
663 haemagglutinating and enzymic activities of Bacteroides fragilis whole cells and outer
664 membrane vesicles. *Microb Pathog* **20**, 191-202 (1996).
665 https://doi.org/10.1006/mpat.1996.0018
666 24 Zakharzhevskaya, N. B. *et al.* Interaction of Bacteroides fragilis Toxin with Outer
667 Membrane Vesicles Reveals New Mechanism of Its Secretion and Delivery. *Front Cell*
668 *Infect Microbiol* **7**, 2 (2017). https://doi.org/10.3389/fcimb.2017.00002
669 25 Sharpe, S. W., Kuehn, M. J. & Mason, K. M. Elicitation of epithelial cell-derived immune
670 effectors by outer membrane vesicles of nontypeable Haemophilus influenzae. *Infect*
671 *Immun* **79**, 4361-4369 (2011). https://doi.org/10.1128/IAI.05332-11

672 26 Round, J. L. *et al.* The Toll-like receptor 2 pathway establishes colonization by a
673 commensal of the human microbiota. *Science* **332**, 974-977 (2011).
674 https://doi.org/10.1126/science.1206095
675 27 Lee, S. M. *et al.* Bacterial colonization factors control specificity and stability of the gut
676 microbiota. *Nature* **501**, 426-429 (2013). https://doi.org/10.1038/nature12447
677 28 Sears, C. L., Geis, A. L. & Housseau, F. Bacteroides fragilis subverts mucosal biology:
678 from symbiont to colon carcinogenesis. *J Clin Invest* **124**, 4166-4172 (2014).
679 https://doi.org/10.1172/JCI72334
680 29 Taglieri, M. *et al.* Colorectal Organoids: Models, Imaging, Omics, Therapy, Immunology,
681 and Ethics. *Cells* **14** (2025). https://doi.org/10.3390/cells14060457
682 30 Sen, A. *et al.* Comprehensive gene expression analysis of organoid-derived healthy
683 human colonic epithelium and cancer cell line stimulated with live probiotic bacteria. *Sci*
684 *Rep* **15**, 22325 (2025). https://doi.org/10.1038/s41598-025-07391-x
685 31 Pierce, J. V., Fellows, J. D., Anderson, D. E. & Bernstein, H. D. A clostripain-like
686 protease plays a major role in generating the secretome of enterotoxigenic Bacteroides
687 fragilis. *Mol Microbiol* **115**, 290-304 (2021). https://doi.org/10.1111/mmi.14616
688 32 Choi, V. M. *et al.* Activation of Bacteroides fragilis toxin by a novel bacterial protease
689 contributes to anaerobic sepsis in mice. *Nat Med* **22**, 563-567 (2016).
690 https://doi.org/10.1038/nm.4077
691 33 Elhenawy, W., Debelyy, M. O. & Feldman, M. F. Preferential packing of acidic
692 glycosidases and proteases into Bacteroides outer membrane vesicles. *MBio* **5**, e00909-
693 00914 (2014). https://doi.org/10.1128/mBio.00909-14
694 34 Zakharzhevskaya, N. B. *et al.* Outer membrane vesicles secreted by pathogenic and
695 nonpathogenic Bacteroides fragilis represent different metabolic activities. *Sci Rep* **7**,
696 5008 (2017). https://doi.org/10.1038/s41598-017-05264-6

697 35 Parikh, K. *et al.* Colonic epithelial cell diversity in health and inflammatory bowel disease.
698 *Nature* **567**, 49-55 (2019). https://doi.org/10.1038/s41586-019-0992-y
699 36 Howe, K. L., Wang, A., Hunter, M. M., Stanton, B. A. & McKay, D. M. TGFbeta down-
700 regulation of the CFTR: a means to limit epithelial chloride secretion. *Exp Cell Res* **298**,
701 473-484 (2004). https://doi.org/10.1016/j.yexcr.2004.04.026
702 37 Maitra, R., Shaw, C. M., Stanton, B. A. & Hamilton, J. W. Increased functional cell
703 surface expression of CFTR and DeltaF508-CFTR by the anthracycline doxorubicin. *Am*
704 *J Physiol Cell Physiol* **280**, C1031-1037 (2001).
705 https://doi.org/10.1152/ajpcell.2001.280.5.C1031
706 38 Maitra, R., Shaw, C. M., Stanton, B. A. & Hamilton, J. W. Functional enhancement of
707 CFTR expression by mitomycin C. *Cell Physiol Biochem* **11**, 93-98 (2001).
708 https://doi.org/10.1159/000047796
709 39 France, M. M. & Turner, J. R. The mucosal barrier at a glance. *J Cell Sci* **130**, 307-314
710 (2017). https://doi.org/10.1242/jcs.193482
711 40 Citi, S. *et al.* A short guide to the tight junction. *J Cell Sci* **137** (2024).
712 https://doi.org/10.1242/jcs.261776
713 41 Sheikh, A. *et al.* Outer membrane vesicles from Bacteroides fragilis contain coding and
714 non-coding small RNA species that modulate inflammatory signaling in intestinal
715 epithelial cells. *bioRxiv* (2025). https://doi.org/10.1101/2025.06.25.661399
716 42 Bomberger, J. M. *et al.* Long-distance delivery of bacterial virulence factors by
717 Pseudomonas aeruginosa outer membrane vesicles. *PLoS Pathog* **5**, e1000382 (2009).
718 https://doi.org/10.1371/journal.ppat.1000382
719 43 Bomberger, J. M. *et al.* A Pseudomonas aeruginosa toxin that hijacks the host ubiquitin
720 proteolytic system. *PLoS Pathog* **7**, e1001325 (2011).
721 https://doi.org/10.1371/journal.ppat.1001325

722 44 Koeppen, K. *et al.* Tobramycin reduces key virulence determinants in the proteome of
723 Pseudomonas aeruginosa outer membrane vesicles. *PLoS One* **14**, e0211290 (2019).
724 https://doi.org/10.1371/journal.pone.0211290
725 45 Kumar, A. *et al.* SLC26A3 (DRA, the Congenital Chloride Diarrhea Gene): A Novel
726 Therapeutic Target for Diarrheal Diseases. *Cell Mol Gastroenterol Hepatol* **19**, 101452
727 (2025). https://doi.org/10.1016/j.jcmgh.2024.101452
728 46 Han, Y. W. *et al.* Interactions between periodontal bacteria and human oral epithelial
729 cells: Fusobacterium nucleatum adheres to and invades epithelial cells. *Infect Immun* **68**,
730 3140-3146 (2000). https://doi.org/10.1128/IAI.68.6.3140-3146.2000
731 47 Antosca, K. M. *et al.* Altered Stool Microbiota of Infants with Cystic Fibrosis Shows a
732 Reduction in Genera Associated with Immune Programming from Birth. *J Bacteriol* **201**
733 (2019). https://doi.org/10.1128/JB.00274-19
734 48 Lee, C. G. *et al.* Bacteroides fragilis Toxin Induces Intestinal Epithelial Cell Secretion of
735 Interleukin-8 by the E-Cadherin/beta-Catenin/NF-kappaB Dependent Pathway.
736 *Biomedicines* **10** (2022). https://doi.org/10.3390/biomedicines10040827
737 49 Choi, J. W., Kim, S. C., Hong, S. H. & Lee, H. J. Secretable Small RNAs via Outer
738 Membrane Vesicles in Periodontal Pathogens. *J Dent Res* **96**, 458-466 (2017).
739 https://doi.org/10.1177/0022034516685071
740 50 Gilmore, W. J. *et al.* Bacteroides fragilis outer membrane vesicles preferentially activate
741 innate immune receptors compared to their parent bacteria. *Front Immunol* **13**, 970725
742 (2022). https://doi.org/10.3389/fimmu.2022.970725
743 51 Stanton, B. A. Extracellular Vesicles and Host-Pathogen Interactions: A Review of Inter-
744 Kingdom Signaling by Small Noncoding RNA. *Genes (Basel)* **12** (2021).
745 https://doi.org/10.3390/genes12071010

746 52 Franco, A. A. The Bacteroides fragilis pathogenicity island is contained in a putative
747 novel conjugative transposon. *J Bacteriol* **186**, 6077-6092 (2004).
748 https://doi.org/10.1128/JB.186.18.6077-6092.2004
749 53 Wu, S. *et al.* A human colonic commensal promotes colon tumorigenesis via activation
750 of T helper type 17 T cell responses. *Nat Med* **15**, 1016-1022 (2009).
751 https://doi.org/10.1038/nm.2015
752 54 Chan, J. L. *et al.* Non-toxigenic Bacteroides fragilis (NTBF) administration reduces
753 bacteria-driven chronic colitis and tumor development independent of polysaccharide A.
754 *Mucosal Immunol* **12**, 164-177 (2019). https://doi.org/10.1038/s41385-018-0085-5
755 55 Bauman, S. J. & Kuehn, M. J. Purification of outer membrane vesicles from
756 Pseudomonas aeruginosa and their activation of an IL-8 response. *Microbes Infect* **8**,
757 2400-2408 (2006). https://doi.org/10.1016/j.micinf.2006.05.001
758 56 Koeppen, K. *et al.* An rRNA fragment in extracellular vesicles secreted by human airway
759 epithelial cells increases the fluoroquinolone sensitivity of P. aeruginosa. *Am J Physiol*
760 *Lung Cell Mol Physiol* **325**, L54-L65 (2023). https://doi.org/10.1152/ajplung.00150.2022
761 57 Stanton, B. A., Coutermarsh, B., Barnaby, R. & Hogan, D. Pseudomonas aeruginosa
762 Reduces VX-809 Stimulated F508del-CFTR Chloride Secretion by Airway Epithelial
763 Cells. *PLoS One* **10**, e0127742 (2015). https://doi.org/10.1371/journal.pone.0127742
764 58 Barnaby, R., Koeppen, K. & Stanton, B. A. Cyclodextrins reduce the ability of
765 Pseudomonas aeruginosa outer-membrane vesicles to reduce CFTR Cl(-) secretion. *Am*
766 *J Physiol Lung Cell Mol Physiol* **316**, L206-L215 (2019).
767 https://doi.org/10.1152/ajplung.00316.2018
768 59 Talebian, L., Coutermarsh, B., Channon, J. Y. & Stanton, B. A. Corr4A and VRT325 do
769 not reduce the inflammatory response to P. aeruginosa in human cystic fibrosis airway
770 epithelial cells. *Cell Physiol Biochem* **23**, 199-204 (2009).
771 https://doi.org/10.1159/000204108

772 60 Stanton, B. A. Effects of Pseudomonas aeruginosa on CFTR chloride secretion and the
773 host immune response. *Am J Physiol Cell Physiol* **312**, C357-C366 (2017).
774 https://doi.org/10.1152/ajpcell.00373.2016
775 61 Welsh, J. A. *et al.* Minimal information for studies of extracellular vesicles (MISEV2023):
776 From basic to advanced approaches. *J Extracell Vesicles* **13**, e12404 (2024).
777 https://doi.org/10.1002/jev2.12404
778 62 Arganda-Carreras, I. *et al.* Trainable Weka Segmentation: a machine learning tool for
779 microscopy pixel classification. *Bioinformatics* **33**, 2424-2426 (2017).
780 https://doi.org/10.1093/bioinformatics/btx180
781 63 Team, R. C. *A language and environment for statistical computing.* (A language and
782 environment for statistical computing, 2017).
783 64 Wickham, H. *ggplot2: Elegant Graphics for Data Analysis.* (Springer-Verlag, 2016).

784